LA-UR-97- 4864

Title: Effects of Localized Holes on Charge Transport, Local Structure and Spin Dynamics in the Metallic State of CMR La(1-x)Ca(x)Mn0(3)

CONF-971201--

Author(s): R.H. Heffner
M.F. Hundley
C.H. Booth

MASTER

Submitted to: MRS 97' Fall Meeting

Los Alamos
NATIONAL LABORATORY

Form No. 836 R5
ST 2629 10/91

DISCLAIMER

EFFECTS OF LOCALIZED HOLES ON CHARGE TRANSPORT, LOCAL STRUCTURE AND SPIN DYNAMICS IN THE METALLIC STATE OF CMR $La_{1-x}Ca_xMnO_3$

R. H. HEFFNER,[1] M.F. HUNDLEY[1] AND C. H. BOOTH[1,2]
[1]Los Alamos National Laboratory, Los Alamos, NM 87545
[2]Physics Department, University of California, Irvine, CA 92697

ABSTRACT

We review resistivity, x-ray-absorption fine-structure (XAFS) and muon spin relaxation (μSR) data which provide clear evidence for localized holes causing polaron distortion and unusual spin dynamics *below* T_C in "colossal magnetoresistive" (CMR) $La_{1-x}Ca_xMnO_3$. Resistivity measurements for x=0.33 under an applied field H have shown that $\ln[\rho(H,T)] \propto -M$, where M is the magnetization. The XAFS data show a similar functional dependence for the polaron distortions on M. The data from these two measurements are interpreted in terms of some fraction of the available holes x remaining localized and some increasing fraction becoming delocalized with increasing M. Finally, this polaron-induced spatial inhomogeneity yields anomalously slow, spatially inhomogeneous spin dynamics below T_C, as shown in the μSR data. These experiments individually probe the charge, lattice and spin degrees of freedom in this CMR system and suggest that the polarons retain some identity even at temperatures significantly below T_C.

INTRODUCTION

In 1954 Volger [1] measured a large magnetoresistance effect near the ferromagnetic transition in $La_{0.8}Sr_{0.2}MnO_3$. At that time the double-exchange theory was being developed by Zener [2], Anderson and Hasegawa [3], and deGennes [4], so the magnetoresistance was loosely attributed to this mechanism. At the time, deGennes [4] pointed out that the theory of double exchange (DE) really should include coupling to the lattice degrees of freedom. About 40 years later, the consequences of such a coupling are now being appreciated. Recently, the magnetoresistance in several related materials was studied [5] in more detail and found to be quite large, prompting the term "colossal" magnetoresistance (CMR). Millis *et al.* [6] recognized CMR was too large to be explained by the DE model without invoking lattice distortions (polarons) in the paramagnetic state. Many subsequent experiments confirmed the existence of both polaron transport [7,8] and local lattice distortions [9,10] that are partially removed in the ferromagnetic state, as well as the expected isotope effect [11]. Moreover, there is mounting evidence that the local lattice distortions play an even bigger role in the transport, possibly dominating the electronic properties over a wide range of temperatures both above and below any magnetic transitions. We review some of these measurements, including those that demonstrate the strong dependence of magnetic field on the resistivity and the local polaron distortions. These data have a remarkably similar functional dependence on the magnetization, as we will show. Moreover, μSR experiments [12] indicate that there are anomalously slow and spatially inhomogeneous spin dynamics in these systems, which can be associated with considerable inhomogeneity in the local magnetic environment. Taken together, these data suggest that there exist regions of the sample in the ferromagnetic state that are essentially still conducting via polaron transport, and that the electronic properties are governed primarily by how much the magnetization can change the relative size of these regions. Regions of various

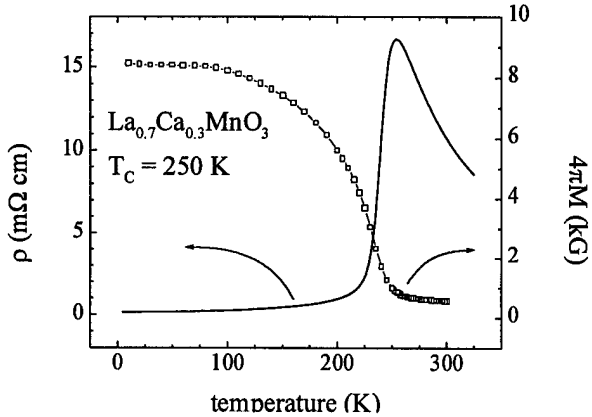

Figure 1: M(T) and ρ(T) for a CMR film with $T_C = 250$ K.

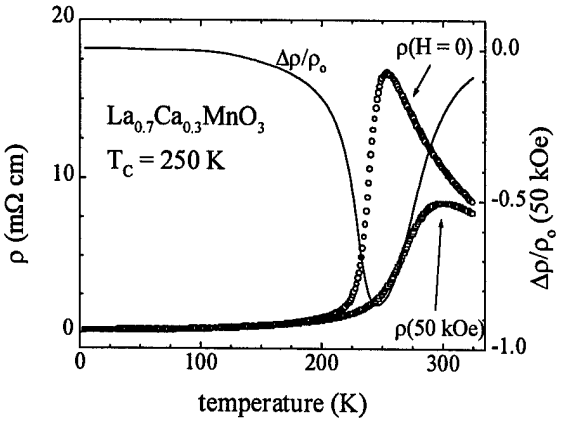

Figure 2: ρ(T) in zero and 50 kOe applied fields (left axis) and transverse MR(T) in 50 kOe (right axis).

sizes can in principle give rise to different spin fluctuation rates. These different regions can also support a wide range of polaron binding energies, consistent with the resistivity and local structure measurements.

DEPENDENCE OF MAGNETIZATION ON RESISTIVITY

The temperature-dependent magnetization and resistivity of an epitaxial thin film of $La_{0.7}Ca_{0.3}MnO_3$ grown via pulsed laser deposition are depicted in Fig. 1. The T-dependent resistivities in zero field and in 50 kOe as well as the resulting magnetoresistance are shown in Fig. 2. The Curie temperature for this specimen was determined to be 250 K from magnetization Arrott plots. For temperatures above T_C, ρ exhibits Arrehenius behavior with an activation energy of 0.1 eV. Hall measurements at 300 K indicate that the carrier concentration is consistent with 0.3 carriers per formula unit and that the drift mobility is only 0.02 cm^2/V-sec, corresponding to a mean-free path that is a fraction of a lattice constant. This clearly indicates that conduction proceeds via nearest-neighbor adiabatic small polaron hopping above T_C. Thermopower and Hall effect measurements confirm that this is indeed the case [13,14]. By applying a 50 kOe magnetic field the peak in ρ at T_C is drastically suppressed and a substantial magnetoresistance is achieved: $\Delta\rho/\rho_o$(50 kOe) = -85% at T_C.

The data in Figs. 1 and 2 show that both $d\rho/dH$ and $d\rho/dT$ are largest near T_C. This region is exactly where dM/dT is a maximum and where an applied magnetic field has the greatest effect on the microscopic magnetism. Thus there is clearly a close connection between charge transport and magnetic order in the manganite CMR compounds. To more fully explore the relationship between ρ and M, careful measurements of $\rho(H,T)$ and $M(H,T)$ were made on the same thin-film sample used to produce the data shown in Figs. 1 and 2. The data were measured at nine temperatures from 272 K to 10 K in fields sufficient to saturate the domain structure so that the measured M would correspond to a microscopic magnetization. The results are presented in Fig. 3 where $\rho(H,T)$ is plotted versus $M(H,T)$ rather than as a function of H or T. The data indicate a correlation that encompasses two orders-of-magnitude variation in ρ and can be parameterized as

$$\rho(H,T) = \rho_m \exp\{-M(H,T)/M_\rho\}, \qquad (1)$$

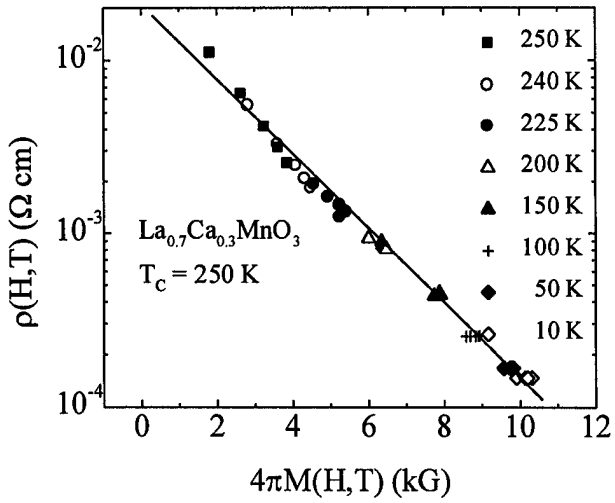

Figure 3: ρ(H,T) plotted as a function of $M(H,T)$. At each temperature points are shown for applied fields of 10, 20, 30, 40, and 50 kOe. The solid line is a least-squares fit to the data.

with ρ_m = 21 mΩ-cm and $4\pi M_\rho$ = 2.0 kG. This resistivity-magnetization correlation was first reported by Hundley *et al.* [7] and has since been confirmed by many others in both thin film [13,15] and bulk samples [12] of CMR compounds with ordering temperatures less than room temperature. Because this correlation appears to hold throughout the temperature range below T_C it is evident that the CMR compounds are not conventional ferromagnetic metals even at low temperatures. Clearly, electronic transport is influenced by magnetic order in a highly unusual way.

By making a few simple assumptions, the phenomenology expressed by Eq. 1 can provide insight into the transport process below T_C. One approach is to assume that the adiabatic small polaron hopping description that is valid above T_C will still apply over a limited temperature range below the ordering temperature. In this scenario, the developing magnetization acts to reduce the polaron binding energy W_P that characterizes the degree to which charge carriers are localized. By following this approach [16] it is straightforward to show that Eq. 1 leads to the simple result that W_P is reduced linearly by the magnetization that develops from either reducing the temperature below T_C or by applying a magnetic field. However, this analysis cannot directly validate the physical picture implied by the adiabatic small polaron theory, namely that W_P is a measure of the spatial extent of the polaron distortion. Consequently, more local experiments, such as a local structure or a local magnetic probe, are necessary to provide a microscopic picture of the transport mechanism.

LOCAL STRUCTURE MEASUREMENTS OF MnO_6 OCTAHEDRA, AND RELATION TO MAGNETIZATION

We now report on local-structure measurements of the MnO_6 distortions in CMR $La_{1-x}Ca_xMnO_3$ and how they relate to the zero-field magnetization. (These measurements are also discussed in Refs. [17,18].) The Mn-O bond length distribution width is measured using the x-ray-absorption fine-structure (XAFS) technique. The measured changes in this width $\Delta\sigma$ due to removal of the polaron distortions below T_C are found to relate to the zero-field magnetization simply as $\ln(\Delta\sigma) \propto M$. Using a simple model whereby each doped hole is either localized

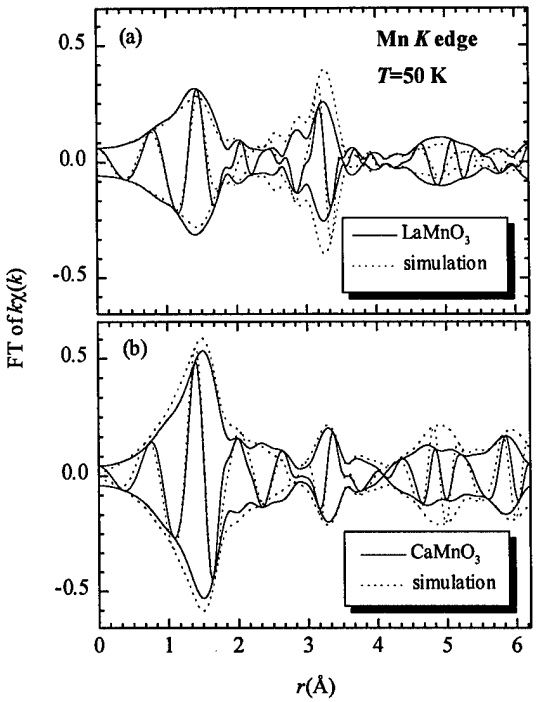

Figure 4: Mn K edge Fourier transforms (FT) of $k\chi(k)$ vs. r for (a) $LaMnO_3$ and (b) $CaMnO_3$ at 50 K. The oscillating curve is the real part and the envelope is the amplitude of the complex transform ($[Re^2+Im^2]^{1/2}$). Dotted lines are from simulations using structures from diffraction, as described in the text.

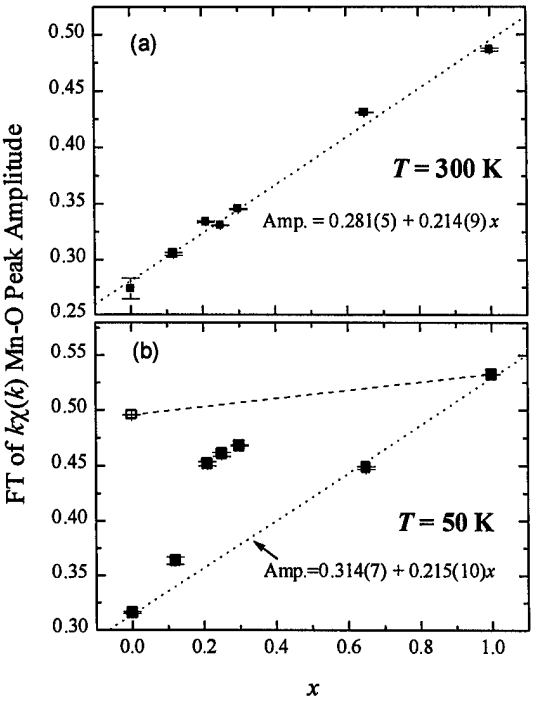

Figure 5: (a) Amplitude of the Mn-O peak in the FT of $k\chi(k)$ at 300 K as a function of x for $La_{1-x}Ca_xMnO_3$. (b) As in (a), except at 50 K. The dotted lines in (a) and (b) are linear fits to the data. The (upper) dashed line is approximately the amplitude one expects if the individual Mn ions were actually mixed valent.

(causing a polaron distortion) or delocalized (causing no polaron distortion), we find that the delocalized hole concentration n_{dh} also changes as $\ln(n_{dh}) \propto M$. This result is in agreement with the dependence of the resistivity on magnetization $\ln(\rho) \propto -M$ shown in Fig. 3. These local structure measurements and the transport measurements therefore provide empirical relations between the spin, charge and lattice degrees of freedom in the Ca-doped CMR manganite perovskites.

The XAFS experiments yield the local structure around a central species of atom, chosen by tuning an incident x-ray beam to a particular absorption edge. For these experiments we measure the absorption region ~900 eV above the Mn K edge. The absorbing photon forces the ejection of a photoelectron with wave vector k given by $E-E_0=\hbar^2k^2/2m_e$, where E_0 is the edge energy and m_e is the electron mass. As the photoelectron is back-scattered from near-neighbor atoms, it interferes with itself at the absorbing atom, causing the absorption coefficient μ to oscillate as $\sin(2kr)$, where r is the distance to the neighboring atom. By isolating the oscillatory part of the absorption (defined as $\chi(k)$), a Fourier transform (FT) of $k\chi(k)$ yields peaks in the amplitude that correspond to the distance (r) between and the number (N) and distribution width (σ) of neighboring atoms. Since the photoelectron back-scattering amplitude $F(k)$ is also a function of k, the FT of $k\chi(k)$ is only *related* to the radial distribution function (RDF). However, $F(k)$ can be calculated to high precision by multiple scattering codes such as FEFF [19], and therefore fits to the FT of $k\chi(k)$ can yield N, r, and σ for the near-neighbor ($< \sim 4.5$ Å) atoms.

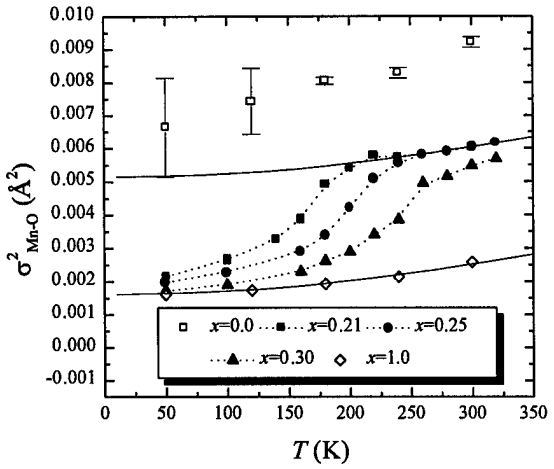

Figure 6: The square of the Mn-O bond length distribution width σ as a function of temperature. The solid line is a fit of the data for $CaMnO_3$ to the correlated-Debye model with Debye temperature Θ_D=940±30 K. This same temperature dependence is also shown with a static of 0.07 Å (upper solid line).

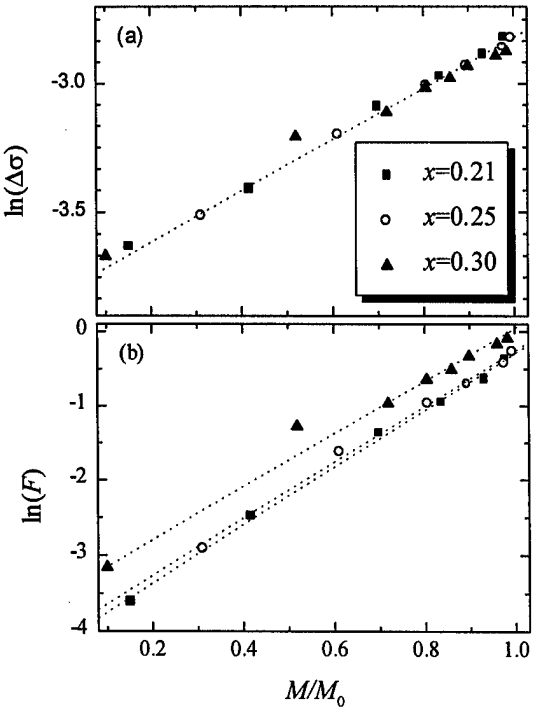

Figure 7: (a) ln(Δσ) as a function of the magnetization. Δσ is the amount of Mn-O bond length distribution width that is removed in the ferromagnetic state for the CMR samples. The magnetization is normalized to the magnetization at T=5 K. (b) ln(F) as a function of the normalized magnetization, as derived for the changes in the local structure. F is the fraction number of delocalolized holes, $F=n_{dh}/x$ (see text).

Fig. 4 shows the FT of $k\chi(k)$ for the end-member compounds $LaMnO_3$ and $CaMnO_3$, together with simulations calculated with FEFF [19], using crystal structures measured by Mitchell *et al.* [20] and Poeppelmeier *et al.* [21], respectively. Considering the large distortions present in both of these compounds (the La/Ca site sits off-center within the perovskite cube, creating a wide range of Mn-La/Ca bond lengths near 3.3 Å), the agreement between the diffraction and XAFS data is remarkably good. One should note that the Mn-O peak at ~1.5 Å (corresponding to Mn-O bond lengths near 1.95 Å) is much lower in amplitude in $LaMnO_3$ than in $CaMnO_3$. This decreased amplitude is a consequence of the Jahn-Teller (JT) distortion that occurs around Mn^{3+} ions. In contrast to the undistorted MnO_6 octahedra in $CaMnO_3$ which gives six Mn-O pairs at ~1.90 Å, the JT distortion causes three distinct bond lengths in $LaMnO_3$, with two oxygen neighbors to the manganese at 1.91 Å, two at 1.97 Å and two at 2.15 Å.

Now we must consider the effect of Ca substitution for La in $LaMnO_3$ on the local Mn-O environment. If each added calcium converts a Mn^{3+} (distorted) into a Mn^{4+} (undistorted) ion, one expects that the amplitude of the Mn-O peak in the FT of $k\chi(k)$ will be linear in the calcium concentration x. This assertion can be verified by simulating such a local environment with FEFF. This linear relation indeed is shown to exist experimentally, as seen in Fig. 5a. Therefore, above T_C, the Mn-O amplitude is an accurate predictor of the *localized* hole concentration.

As we drop below T_C, samples with $0.2<x<0.5$ undergo an insulator-to-metal (CMR) transition, together with a (partial) removal of the JT distortion of the MnO_6 octahedra. Samples

outside of this concentration range remain insulating, regardless of their magnetic state. For such samples, the linear relationship between x and Mn-O peak amplitude still holds, while for the CMR samples, the peak amplitude is higher than the line describing the non-CMR samples (Fig. 5b). If the distortion were completely removed, one might expect the Mn-O peak to be undistorted. The *lowest* amplitude that could be expected would be determined from the sum of the $Mn^{(3+x)+}$ and O^{2-} ionic radii, and is roughly shown as the (upper) dashed line in Fig. 5b. (XAFS amplitudes decrease with increasing r.) The real amplitudes for the CMR materials fall well below the line describing the undistorted case, and therefore significant distortions still exist, even well below T_C.

To quantify these effects with temperature, we have performed fits to the XAFS spectra, using a Gaussian distribution of six Mn-O bonds, with a bond-length distribution width σ. These Mn-O widths are displayed in Fig. 6, showing only the CMR samples and the end-members of the $La_{1-x}Ca_xMnO_3$ series for clarity. The other (non-CMR) samples show little or no change in σ at their magnetic transitions, and their magnitudes are given roughly by interpolating $1/\sigma$ between the end members.

The polaron contribution to the total width can be isolated and compared to the zero-field magnetization. The total width σ above T_C can be written as the sum (in quadrature) of a thermal (Debye) contribution σ_D and the fully-developed (static) polaron contribution σ_P: $\sigma=(\sigma_D^2+\sigma_P^2)^{1/2}$. For these data, we determine σ_D by fitting the data for $CaMnO_3$ and adding a static σ_P, as shown in Fig. 6. The thermal dependence of σ above T_C in the CMR materials appears to agree well with the data for $CaMnO_3$. Below T_C, the change in the width due the finite magnetization can be written as $\Delta\sigma=(\sigma^2-\sigma_D^2+\sigma_P^2)^{1/2}$. The zero-field magnetization can be estimated by the SQUID-measured magnetization M normalized to the low temperature magnetization M_0. (Magnetization measurements are reported in Ref. [17,18].)

Fig. 7a demonstrates that $\ln(\Delta\sigma) \propto M/M_0$, with all the data from this small sample set falling on the same line. This relationship strongly supports the existence of the JT distortions below T_C, and shows how they develop with decreasing magnetization, and thus increasing temperature. These data are in agreement with PDF data on the related $La_{1-x}Sr_xMnO_3$ system which demonstrate the existence of JT distortions below T_C for $x< \sim 0.35$ [22]. It is important that such a relationship is calculable within a double-exchange theory that includes polarons [23], and thus may provide an important test of such theories [24,25].

A "two-fluid" model of the Mn-O distortions and the conductivity

A simple "two fluid" model can describe these data as well. Consider that in the metallic state each of the doped holes x can be either in a localized (non-conducting) or a delocalized (conducting) state. Such a model ignores the effect of changes in the carrier mobility on the structure, such as may occur if the states become only partially extended. With this assumption, we can model the effect of the distortions that we measure by assuming that each localized charge will create a Mn^{3+} site and a JT distortion around that site. This model exactly describes the linear relationship in the paramagnetic state shown in Fig. 5a. When the material becomes ferromagnetic, some fraction of the holes become delocalized and no longer contributes to the lattice distortion. In the limit of no distortion, the width of the peak should be the same as $CaMnO_3$. With such a simple distribution of distortions, we can immediately write down the delocalized hole concentration n_{dh}. In terms of distribution amplitudes (which are slightly different that the amplitude of the FT of $k\chi(k)$ in Fig.5 [18]), n_{dh} is given by the difference between the measured amplitude A and the amplitude one expects if the distortion remains fully developed A_D, normalized by the difference between the amplitude expected for no distortion

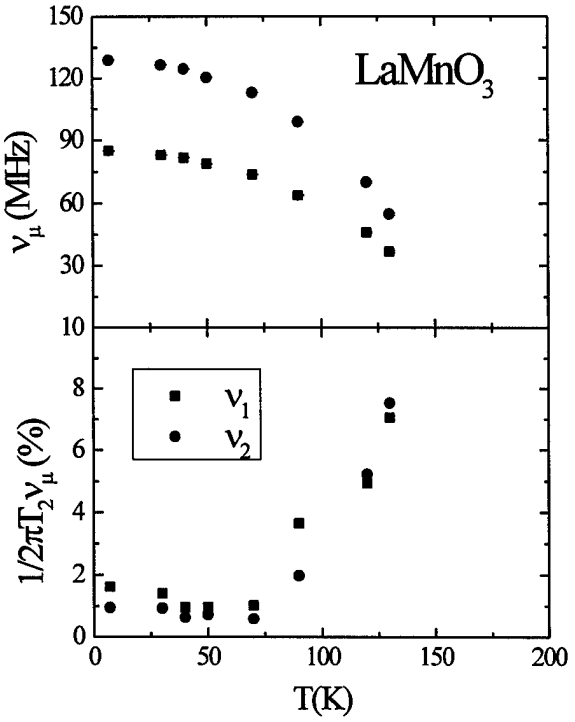

Figure 8: Temperature dependence of the μSR frequency (upper panel), proportional to the sublattice magnetization, in $LaMnO_3$. Temperature dependence of the inhomogeneous linewidth $1/T_2$ divided by the precession frequency ω_μ.

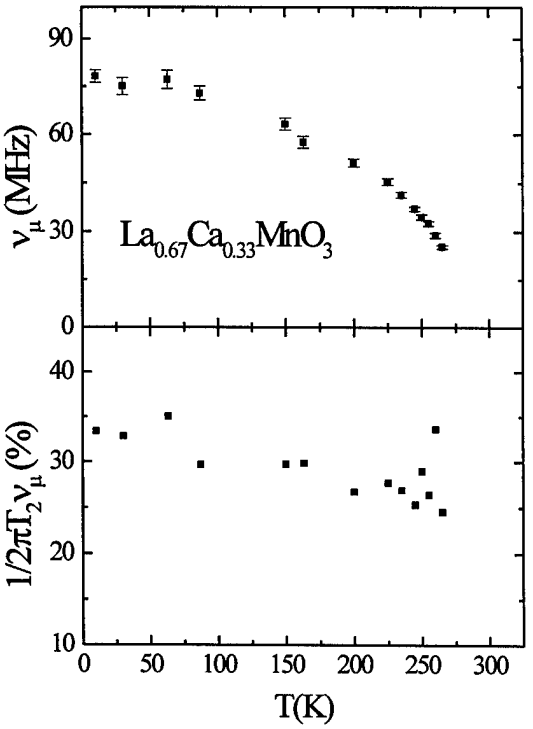

Figure 9: Temperature dependence of the μSR frequency (upper panel), proportional to the sublattice magnetization, in $La_{0.67}Ca_{0.33}MnO_3$. Temperature dependence of the inhomogeneous linewidth $1/T_2$ divided by the precession frequency ω_μ.

A_{ND} and A_D. These amplitudes are given by the number of Mn-O neighbors (six) times $(2\pi\sigma^2)^{-1/2}$. We may therefore write

$$n_{dh} = \frac{A(x,T,M) - A_D(x,T)}{A_{ND}(x,T) - A_D(x,T)} = \frac{1/\sigma - 1/\sigma_D}{1/\sigma_{ND} - 1/\sigma_D} \qquad (2)$$

A plot of the fractional number of delocalized holes $F = n_{dh}/x$ determined in this fashion is shown in Fig. 7b. Again, $\ln(F) \propto M$. Using fits to these data, one also finds that even at T=0, not all the holes in these samples are completely delocalized: $n_{dh}(T=0)/x$ goes from 0.77→0.86 for x=0.21→0.30. We do not have a good explanation of this change in $n_{dh}(0)$, but it may be related to the number of cation vacancies in these samples.

ANOMALOUSLY SLOW, INHOMOGENEOUS SPIN DYNAMICS BELOW T_C FROM μSR

The XAFS data described above present strong evidence for significant average lattice distortions at temperatures far below T_C, which in turn is associated with charge localization.

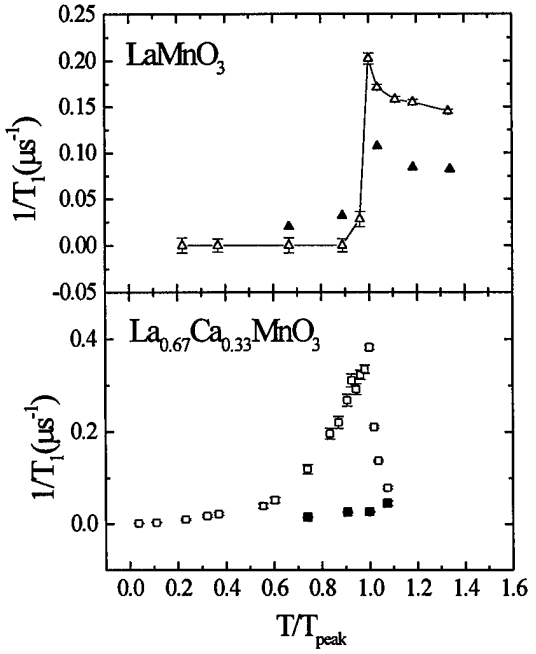

Figure 10: Temperature dependence of the μSR spin lattice relaxation rate $1/T_1$ in $LaMnO_3$ (upper panel) and $La_{0.67}Ca_{0.33}MnO_3$ lower panel. The open symbols are for zero applied field and the closed symbols are for 3 kOe applied field.

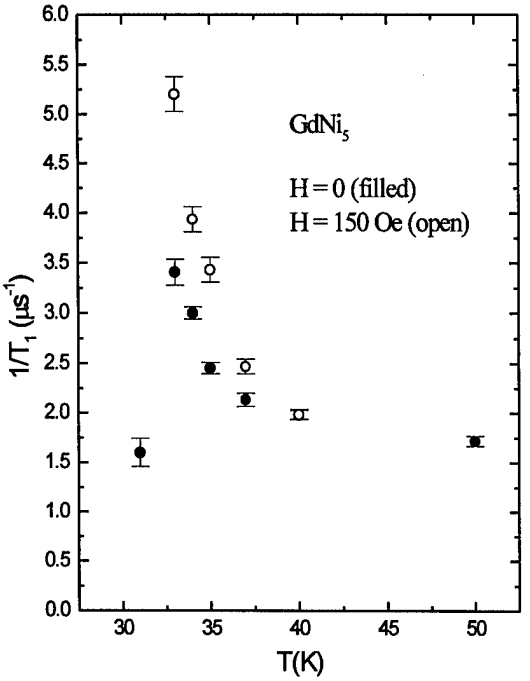

Figure 11: Temperature dependence of the μSR rate $1/T_1$ in the Heisenberg ferromagnet $GdNi_5$ ($T_C \cong 32$ K).

The clear connection between the residual distortion, the overall sample magnetization and the resistivity relates the microscopic lattice degrees of freedom to the *macroscopic* charge and spin degrees of freedom. This correlation with the spin degrees of freedom can be explored *microscopically* using the muon spin relaxation (μSR) technique. Here 100% spin polarized muons are implanted interstitially and the relaxation of the muons' polarization in time is detected by monitoring the anisotropy in the direction of the emitted decay positrons. This leads to a relaxation function that is given [12] by the formula

$$G_z(t) = A_1 \exp(-(t/T_1)^K) + A_2 \exp(-t/T_2) \cos(2\pi\nu_\mu t + \phi). \quad (3)$$

Here T_1^{-1} and T_2^{-1} are the respective homogeneous and inhomogeneous linewidths, $\omega_\mu = 2\pi\nu_\mu = \gamma_\mu |B|$ is the muon Larmor precession frequency in the internal field B, and A_1 and A_2 are the relative amplitudes of the fluctuating and precessing components of the local field, respectively. The above assumes a single muon magnetic environment, so that $A_1 + A_2 = 1$.

Figs. 8 and 9 show the temperature dependence of the muon frequency ν_μ and the fractional linewidth $1/(2\pi T_2\nu_\mu)$ in both $LaMnO_3$ and $La_{0.67}Ca_{0.33}MnO_3$. The ν_μ values are proportional to the local sublattice magnetization. There are two frequencies found in $LaMnO_3$, corresponding to two magnetically inequivalent muon sites in the antiferromagnetic structure. Only a single muon line is observed in the doped material, indicating a single interstitial site. In an earlier publication [12] we showed that the temperature dependence of ν_μ in $La_{0.67}Ca_{0.33}MnO_3$ is well described by the functional form expected for a second order phase transition $\nu_\mu = \nu_0(1-T/T_C)^{1/3}$. Both of the lines for $LaMnO_3$ are fit by this same expression, but with an

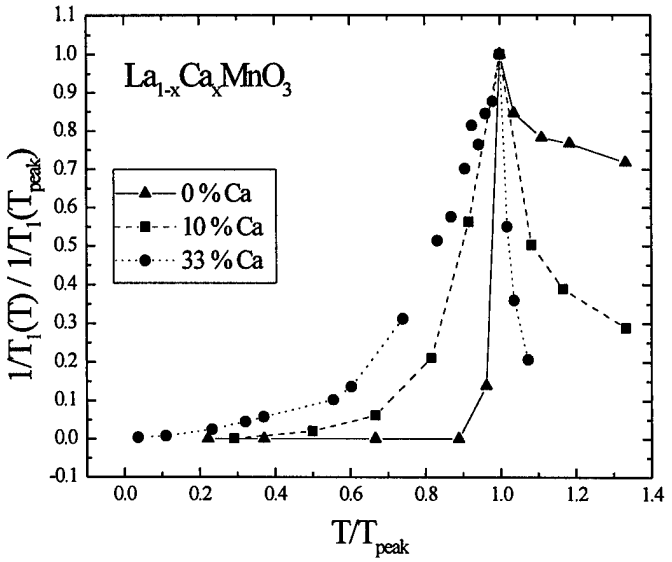

Figure 12: Temperature dependence of the spin lattice relaxation rate $1/T_1$ in $La_{1-x}Ca_xMnO_3$. The x-axis has been normalized to the magnetic ordering temperature and the y-axis to the maximum relaxation rate in each sample.

exponent of about 0.29. The lower panel in Fig. 8 shows that the inhomogeneous linewidth in the undoped sample is quite narrow, except near T_N. By contrast, in $La_{0.67}Ca_{0.33}MnO_3$ (lower panel, Fig. 9) the linewidth tracks the sublattice magnetization and is at least an order of magnitude larger than in the undoped material. In this case both the magnitude and temperature dependence (proportional to the magnetization) of the linewidth suggest that its origin comes from a distribution of grain shapes in the polycrystalline sample, giving rise to a distribution of demagnetization factors. We return to this point below.

Fig. 10 shows the temperature dependence of the spin lattice relaxation rates in $LaMnO_3$ and $La_{0.67}Ca_{0.33}MnO_3$. The open and closed symbols are for zero and 3 kOe applied field, respectively. One expects almost no relaxation below the ordering temperature in magnets with appreciable spin stiffness constants [26]. This is because $1/T_1$ is usually dominated by two-magnon relaxation from spin waves, which is proportional to $T(\ln T)/D^3$, where D is the spin wave stiffness [26]. The stiffness constant in the manganites is indeed large enough that no relaxation from the spin waves is expected ($D \cong 155$ meV Å^2 in $La_{0.67}Ca_{0.33}MnO_3$). This is what is observed in $LaMnO_3$; i.e., no appreciable μSR rate is observed below T_N. However, in the Ca-doped material the relaxation below T_C is appreciable and is attributed to the effects of spin-lattice polarons, as discussed below. An important point to note is that $1/T_1 \propto \Delta^2 \tau$, where Δ is the amplitude of the fluctuating hyperfine field and τ is the correlation time of the fluctuations. Thus anomalously slow fluctuation rates or long correlation times τ are associated with the relaxation below T_C in $La_{0.67}Ca_{0.33}MnO_3$.

These anomalously slow fluctuations produce a μSR rate that is very sensitive to an applied field, as seen in Fig. 10. Whereas a field of only 3 kOe completely destroys the peak in the relaxation rate for $La_{0.67}Ca_{0.33}MnO_3$, one still sees the relaxation peak in the antiferromagnet $LaMnO_3$. Although one would expect an applied field to couple more strongly to a ferromagnet than an antiferromagnet, fields of comparable sizes in other ferromagnetic materials do not have such a drastic effect. This is seen in the case of $GdNi_5$, a typical Heisenberg ferromagnet, shown

in Fig. 11. The application of a small field actually enhances the relaxation rates near T_C presumably because the field slows down the fluctuations.

We have also performed measurements on the material $La_{0.90}Ca_{0.10}MnO_3$, which lies in a region of the phase diagram where canted antiferromagnetic order has been suggested [27] (i.e., ferromagnetism is just beginning to develop). A comparison of the relaxation rates for the three systems with $x = 0.0$, 0.10 and 0.33 is shown in Fig. 12, where the axes have been normalized. One notes that the relaxation below the ordering temperature increases in magnitude relative to its peak rate as the system is doped with Ca. Thus the presence of doped holes (and presumably their associated spin-lattice polarons) is responsible for the anomalously slow relaxation below T_C.

A detailed analysis of the dynamical component (the A_1 component in Eq. 3) of the relaxation function $G_z(t)$ reveals that it has a stretched-exponential form below and slightly above T_C, with an exponent $K \leq ½$. In the ferromagnetic compound $GdNi_5$ discussed above, as well as in the random ferromagnet Pd*Mn* (2%) [28], the relaxation function is exponential above and below T_C. A stretched exponential relaxation function implies that there exists a broad distribution of relaxation rates $1/T_1$, leading to the conclusion that Δ and/or τ are distributed quantities.

To understand how a distribution in Δ affects the measured relaxation function we convoluted both a Gaussian and a Lorentzian broadening function $P(\Delta)$ with the exponential relaxation function $\exp(-t/T_1)$, i.e.,

$$\exp(-(t/T_1)^K) = \int d\Delta\, P(\Delta)\exp(-t/T_1). \qquad (4)$$

Using the value obtained from the inhomogeneous linewidth shown in Fig. 9 (lower panel) as an upper limit for Δ, we find that $K \geq 0.6$. Obviously, the smaller the value of Δ the larger the value of K, i.e., $K = 1$ for $\Delta = 0$. Recall that the physical meaning of Δ is the amplitude of the fluctuating hyperfine field produced by the Mn spins at the muon site. Thus the actual value of Δ for our experiment in $La_{0.67}Ca_{0.33}MnO_3$ is likely to be much smaller than the value obtained from the inhomogeneous linewidth $1/T_2$, which is presumably dominated by a distribution of demagnetizing fields from the various grain shapes in the sample. Consequently, the measured exponent K cannot be explained by a spread in the intrinsic Δ values alone, strongly suggesting that the local-field correlation time τ is also a distributed quantity. Because μSR is a local probe one may therefore infer that the fluctuations are spatially inhomogeneous.

In summary, the principle findings from μSR are that the spin fluctuations below T_C in $La_{0.67}Ca_{0.33}MnO_3$ are anomalously slow, spatially inhomogeneous and very sensitive to small-applied fields. These results can be related to the combined XAFS, resistivity and magnetization experiments by assuming that the small polarons observed previously in transport measurements above T_C retain some identity in the ferromagnetic state; i.e., the system is not homogeneous below T_C. The presence of structural inhomogeneity below T_C is quite clear from the XAFS measurements, and as discussed above, this can be related to the existence of both localized and delocalized charges. The μSR measurements likewise indicate inhomogeneity, but in the fluctuations of the Mn spins.

To reconcile these results we hypothesize that the regions of localized and delocalized charge (or alternatively, regions of large and small local lattice distortion) produce spin clusters of varying sizes and that the fluctuation rates within a cluster depend on the cluster size. This gives rise to a distribution of relatively slow fluctuation rates (we find $1/\tau \leq 10^{-11}$ s^{-1} near and below T_C). One may estimate an upper limit for the cluster size by noting that when the spin cluster or polaron reaches the size of the ferromagnetic coherence length it can support spin

waves, which do not relax the muon spin, as discussed above. Estimates of this correlation length are ≥ 15- 20 Å [29]. A reasonable lower limit for the cluster size is 1-2 lattice spacings, slightly larger that the expected size of the small polarons in the paramagnetic state. The unusual field dependence observed for the μSR relaxation rate could thus be explained by postulating that a small field will enlarge the cluster size a few lattice spacings (by enhancing the charge transport which is mediated through the double exchange) until spin waves are again supported locally. Note that a much larger field is required to significantly reduce the resistivity, where charge must be transported across the entire sample.

In conclusion, we have presented three different types of measurements that separately probe the charge, lattice and spin degrees of freedom in the Ca-doped CMR manganites. As expected, the transport, local structure, and μSR measurements show clear evidence for the presence of small polarons both in the electronic properties and from the Jahn-Teller distortions in the paramagnetic state. What is surprising is that these measurements provide compelling evidence that even well below T_C, there are still signatures of local lattice distortions and other polaron-like effects, albeit diminished from those observed above T_C. Taken together, these experiments are consistent with a model wherein regions of the sample display small spin-lattice polaron dynamics and that these regions continuously change into regions with free-carrier-like dynamics below the magnetic ordering temperature. The presence of polarons and the dramatic effect they have on the transport, structure and magnetic properties indicates that these compounds are *not* simple ferromagnetic metals well below T_C and any description of the underlying physical mechanism responsible for their unique properties must account for this fact. These measurements therefore provide an important glimpse into the nature of the ground-state in CMR compounds.

ACKNOWLEDGEMENTS

The authors thank A. Millis for useful discussions. Work at Los Alamos National Laboratory (LANL) was performed under the auspices of the U.S. Department of Energy (DOE), and supported in part by funds provided by the University of California for the conduct of discretionary research by LANL. The XAFS experiments were performed at the Stanford Synchrotron Radiation Laboratory, which is operated by the DOE, Division of Chemical Sciences, and by the NIH, Biomedical Resource Technology Program, Division of Research Resources.

References

1. J. Volger, Physica **20**, 49 (1954).
2. C. Zener, Phys. Rev. **82**, 403 (1951).
3. P. W. Anderson and H. Hasegawa, Phys. Rev. **100**, 675 (1955).
4. P. G. deGennes, Phys. Rev. **118**, 141 (1960).
5. R. M. Kusters, J. Singleton, D. A. Keen, R. McGreevy, and W. Hayes, Physica B **155**, 362 (1989); K. Chahara, T. Ohuo, M. Kasai, and Y. Kozono, Appl. Phys. Lett. **63**, 1990 (1993); R. von Helmholt, J. Wecker, B. Holzapfel, L. Schultz, and K. Samwer, Phys. Rev. Lett. **71**, 2331 (1993); S. Jin, M. McCormack, T. H. Tiefel, R. M. Fleming, J. Phillips, and T. Ramesh, Science **264**, 413 (1994).
6. A. J. Millis, P. B. Littlewood, and B. I. Shraiman, Phys. Rev. Lett. **74**, 5144 (1995).
7. M. F. Hundley, M. Hawley, R. H. Heffner, Q. X. Jia, J. J. Neumeier, J. Tesmer, X. D. Wu, and J. D. Thompson, Appl. Phys. Lett. **67**, 860 (1995).

8. M. Jaime, M. B. Salamon, M. Rubinstein, R. E. Treece, J. S. Horwitz, and D. B. Chrisey, Appl. Phys. Lett., **68**, 1576 (1996).
9. S. J. L. Billinge, R. G. DiFrancesco, G. H. Kwei, J. J. Neumeier, and J. D. Thompson, Phys. Rev. Lett. **77**, 715 (1996).
10. C. H. Booth, F. Bridges, G. J. Snyder, and T. H. Geballe, Phys. Rev. B **54**, R15606 (1996).
11. G. Zhao, K. Conder, H. Keller, and K. A. Müller, Nature **381**, 676 (1996).
12. R.H. Heffner, L.P. Le, M.F. Hundley, J.J. Neumeier, G.M. Luke, K. Kojima, B. Nachumi, Y.J. Uemura, D.E. MacLaughlin, and S-W. Cheong, Phys. Rev. Lett. **77**, 1869 (1996).
13. M. Jaime, M.B. Salamon, M. Rubinstein, R.E. Treece, J.S. Horwitz, and D.B. Chrisey, Phys. Rev. B **54**, 11914 (1996).
14. M. Jaime, H.T. Hardner, M.B. Salamon, M. Rubinstein, P. Dorsey, and D. Emin, Phys. Rev. Lett. **78**, 951 (1997); M.F. Hundley and J.J. Neumeier, Phys. Rev. B **55**, 11511 (1997).
15. J.Z. Sun, L. Krusin-Elbaum, S.S.P. Parkin, and Gang Xiao, Appl. Phys. Lett. **67**, 2726 (1995); B.X. Chen, C. Uher, D.T. Morelli, J.V. Mantese, A.M. Mance, and A.L. Micheli, Phys. Rev. B **53**, 5094 (1996); B. Martinez, J. Fontcuberta, A. Seffar, J.L. Garcia-muñoz, S. Piñol, and X. Obradors, Phys. Rev. B ***54***, 10001 (1996).
16. M.F. Hundley, J.J. Neumeier, R.H. Heffner, Q.X. Jia, X.D. Wu, and J.D. Thompson in Epitaxial Oxide Thin Films III, edited by D.G. Schlom, C-B. Eom, M.E. Hawley, C.M. Foster, and J.S. Speck (Mater. Res. Soc. Proc. 474, Pittsburgh, PA 1997), p. 167.
17. C. H. Booth, F. Bridges, G. H. Kwei, J. M. Lawrence, A. L. Cornelius, and J. J. Neumeier, Phys. Rev. Lett., in press.
18. C. H. Booth, F. Bridges, G. H. Kwei, J. M. Lawrence, A. L. Cornelius, and J. J. Neumeier, submitted to Phys. Rev. B.
19. S. I. Zabinsky, A. Ankudinov, J. J. Rehr, and R. C. Albers, Phys. Rev. B **52**, 2995 (1995).
20. J. F. Mitchell *et al.*, Phys. Rev. B **54**, 6172 (1996).
21. K. R. Poeppelmeier, M. E. Leonowicz, J. C. Scanlon, and J. M. Longo, J. Solid State Chem. **45**, 71 (1982).
22. D. Louca, W. Dmowski, T. Egami, E. L. Brosha, H. Röder, and A. R. Bishop, Phys. Rev. B 56, R8475 (1997).
23. A. J. Millis and H. Röder, private communication.
24. A. J. Millis, R. Mueller, and B. I. Shraiman, Phys. Rev. B **54**, 5405 (1996).
25. H. Röder, J. Zang, and A. R. Bishop, Phys. Rev. Lett. **76**, 1356 (1996).
26. A. Yaouanc and P. Dalmas de Réotier, J. Phys.: Cond. Matter **3**, 6195 (1991).
27. E. O. Wollen and W. C. Koehler, Phys. Rev. **100**, 548 (1995).
28. S. A. Dodds, G. A. Gist, D. E. MacLaughlin, R. H. Heffner, M. Leon, M. E. Schillaci, G. J. Nieuwenhuys and J. A. Mydosh, Phys. Rev. B **28**, 6209 (1983).
29. J. W. Lynn, R. W. Erwin, J. A. Borchers, Q. Huang, A. Santoro, J.-L. Peng, and Z. Y. Li, Phys. Rev. Lett. **76**, 4046 (1996).

Report Number (14) LA-UR--97-4864
CONF-971201--

Publ. Date (11) 199803
Sponsor Code (18) DOE/MA, XF
UC Category (19) UC-904, DOE/ER

DOE